Application of high concentration thulium-doped fiber for achieving S-band gain flattened hybrid optical amplifier

S. D. EMAMI[a*], P. HAJIREZA[b], F. ABD-RAHMAN[b], H. A. ABDUL-RASHID[b], H. AHMAD[c], S. W. HARUN[a]
[a]*Department of Electrical Engineering, University of Malaya 50603 Kuala Lumpur, Malaysia.*
[b]*Faculty of Engineering, Multimedia University, 63100 Cyberjaya, Malaysia*
[c]*Photonics Research Center, University of Malaya 50603 Kuala Lumpur, Malaysia*

A hybrid amplifier is proposed using a series configuration of Thulium-doped fiber (TDF) and Raman amplifiers, which shares the same pump laser. This amplifier covers the bandwidth of entire short wavelength band (S-band) region by combining the gain spectrum of the TDF and Raman amplifiers. The new method of gain flattening is suggested by adding a second stage amplifier with a high concentration TDF as a gain medium. The flat gain is theoretically obtained at around 24dB. The development of reliable high-power diode lasers in the 1420 nm wavelength range will make this type of wide-band hybrid amplifier an interesting candidate for S-band optical telecommunication systems.

1. Introduction

Due to the tremendous increase in communication traffic in recent years, more and more efforts in research have been directed towards developing highly efficient fiber amplifiers that operates in wider bandwidth [1-3]. One of the effective ways to extend the gain bandwidth of the optical amplifiers is to use a hybrid configuration of several amplifiers with different gain bandwidths. Connecting the amplifier in parallel or in series are methods that has been used to achieve a wide-band amplifier [4]. In case of parallel configuration, the input signal is first de-multiplexed into different band by the wavelength division multiplexing (WDM) coupler, amplified by amplifiers that are suitable for the corresponding wavelength band, and finally multiplexed again with a WDM coupler. This type of hybrid amplifier has the advantage of extensibility, in which one amplifier can initially work independently while another amplifier can be added into the system according to the capacity demand expansion. Unusable wavelength region exists between each gain band originated from the guard band of the WDM coupler is the main disadvantages of the parallel type of hybrid amplifier [5]. The noise figure of this amplifier also increases due to the insertion loss of the WDM coupler, which is located at the input end of each amplifier. To cope with this problem, the hybrid amplifier is connected in series to avoid the use of the WDM coupler [6].

However, non-uniform gain profile is still one of the main disadvantages of the hybrid amplifiers, which cause some channels to be amplified preferentially at the expense of attenuating other channels. This non-uniform gain spectral profile results in a serious reduction of gain bandwidth when amplifiers are cascaded in transmission links. To address this problem, a hybrid amplifier is developed by shifting the gain spectrum of TDFA to longer wavelengths by using high concentration TDF. This gain shifted TDFA provides a noise figure as low as 3 dB but suffers from a low 11% optical-to-optical conversion efficiency (defined as amplifier output power divided by total pump power) [6].

In this paper, gain flattened hybrid TDFA and fiber Raman amplifier (FRA) operating in S-band region is proposed and demonstrated using a gain shifting technique. This hybrid amplifier cascades a two-stage TDFA with two pieces of TDFs with different Thulium concentrations of 2000 ppm and 6000 ppm and FRA in series. First, we describe spectroscopic considerations of thulium ions and the concept of gain shifting. Then, numerical modeling of TDFA based on comprehensive rate equation is described and analyzed. Next, we report the amplification characteristics of fiber Raman amplifier. Then the gain and noise characteristics of the hybrid amplifier with and without an incorporation of high concentration TDF are theoretically investigated. The proposed amplifier uses only a single 1420 nm pump laser to pump both linear and nonlinear gain media. Theoretical calculations were verified by previously reported experimental results [6, 7].

2. Thulium spectroscopic profile

Fig. 1 shows the energy level diagram of the TDFA in low-phonon-energy fluoride glasses. The variables N_0, N_1,

N_2 and N_3 are used to represent population of ions in the $^3H_6$, $^3F_4$, $^3H_5$ and $^3H_4$ energy levels respectively. The main transition used for S-band amplification is from the $^3F_4$ (the upper laser level) to $^3H_4$ energy levels (the lower laser level). Stimulated emission from $^3F_4$ to $^3H_4$ emits photons at 1380–1550 nm with a peak at 1460 nm [8, 9]. One of the common methods for pumping in TDFA is using 1420 nm up-conversion pump. The 1420 nm pump is used for ground state absorption (1st stage pumping from $^3H_6$ to $^3H_4$) and also excited state absorption (ESA, 2nd stage pumping from $^3H_4$ to $^3F_4$). With 1420nm pumping, the thulium ions are excited from the ground-state, $^3H_6$ to $^3H_4$ energy level and then are further excited to the upper energy state ($^3F_4$) via the ESA [8]. This creates a population inversion between the $^3H_4$ to $^3F_4$ energy levels, which allows S-band amplification via stimulated emission.
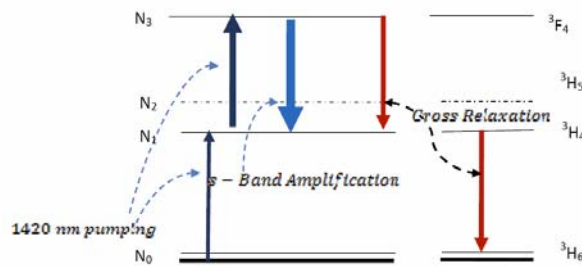

Fig. 1. Up-conversion pumping scheme of 1420 nm.

An amplified spontaneous emission (ASE) spectrum for transition between $^3H_4$ to $^3F_4$ level peaks at around 1460 nm [10]. Fig. 2 shows the gain spectrum at various fractional inversions in the TDF [10]. Low fractional inversion (typically 0.4) is the main key for achieving gain shifting in fiber amplifiers. Fractional inversion in TDF is defined as $\Delta N = N_3/ (N_1+N_3)$. The equation of gain per unit length as a function of wavelength can be defined as GPL $(\lambda) = N_3\sigma_{se} - N_1\sigma_{sa}$, where σ_{se} and σ_{se} are the emission and absorption cross-sections between the N_3 and N_1 levels, respectively [11, 12]. As shown in Fig. 2, the TDFA gain peaks at 1460nm if the fractional inversion is larger than 0.7 while low fractional inversion around 0.4 provides gain-shifted operation whose peak is located at 1500 m. For achieving low fractional inversion, many methods have been reported such as using an EDF with a very high Thulium concentration [13]. By using high concentration thulium, cross relaxation occurs between the thulium ions. Energy of thulium ion which is excited at the $^3H_4$ level transfers to a neighboring thulium ion in the ground state level, and both ions enter the $^3F_4$ meta-stable state. Result of this level energy transfer cause that the amount of population ion at N_1 level becomes high, which means that the population inversion state between the $^3H_4$ and $^3F_4$ levels becomes lower than 40% [12].
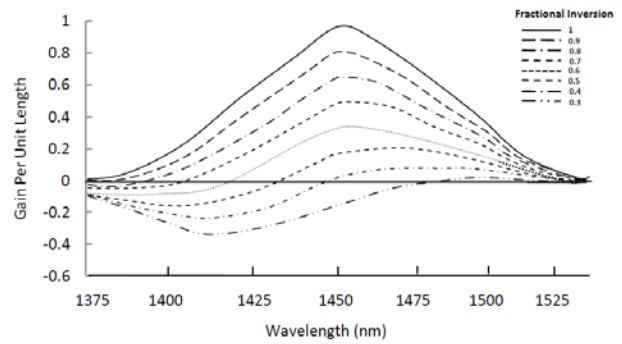

Fig. 2. Gain per unit length spectra [10].

3. Configuration of the hybrid amplifier

The configurations of the hybrid amplifier with single-stage and two-stage TDF are shown in Fig. 3(a) and 3(b), respectively, in which the TDFs and Raman amplifier are cascaded in series with same pump laser wavelength. 1420 nm pump lasers are used as the pump source for all amplifiers. A 20 m long TDF with thulium ion concentration of 2000 ppm is used in the first stage and a 10 km long dispersion compensating fiber (DCF) is used as a Raman gain medium in both configurations. For the proposed configuration of Fig. 3(b), another TDFA with 4 m long TDF of 6000 ppm Thulium concentration is added in the configuration to allow gain shifting.
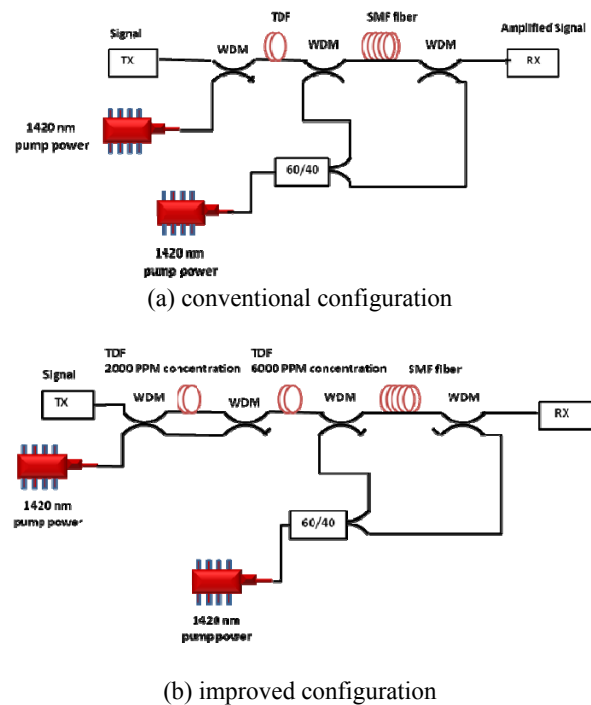

(a) conventional configuration

(b) improved configuration

Fig. 3. Configurations of the hybrid TDFA/FRA

4. Mathematical Model of the TDFA

Fig. 4 shows the pump signal and ASE transition of TDFA which demonstrates a radiative and non-radiative transition in TDF. According to this figure, the rate equation for the ion population at each layer of single pass TDFA can be written as [8];

$$\frac{dN_0}{dt} = -(W_{p01} + W_{18a} + W_{8a})N_0 + (A_{10} + W_{18e})N_1 + (A_{30} + W_{8e})N_3 \tag{1}$$

$$\frac{dN_1}{dt} = (W_{18a} + W_{p01})N_0 - (A_{10} + W_{p13} + W_{Sa} + W_{18e})N_1 + (W_{p31} + W_{Se} + A_{31})N_3 \tag{2}$$

$$\frac{dN_3}{dt} = (W_{8a})N_0 + (W_{p13} + W_{Sa})N_1 - (A_{30} + A_{31} + W_{p31} + W_{se} + W_{8e})N_3 \tag{3}$$

$$\sum_i N_i = \rho \tag{4}$$

where W_{p01}, W_{p13} and W_{p31} are transition rates of the 1420 nm pump. Signal stimulated absorption and emission are described by W_{sa} and W_{se} respectively. The transition rates of amplified spontaneous emission (ASE) at 800 nm ($^3H_4 \rightarrow {}^3H_6$) and 1800 nm ($^3F_4 \rightarrow {}^3H_6$) are governed by W_{8e}, W_{18e}, respectively. The transition rates of stimulated absorption at 800 nm ($^3H_4 \rightarrow {}^3H_6$) and 1800 nm ($^3F_4 \rightarrow {}^3H_6$) are governed by W_{8a}, W_{18a} respectively. A_{ij} is the radiative rate from level i to level j. Others radiative transitions are not included in the rate equations because they have an ignorable effect on the S-band amplification. Transition rates of the pump, stimulated absorption and stimulated emission are given by:
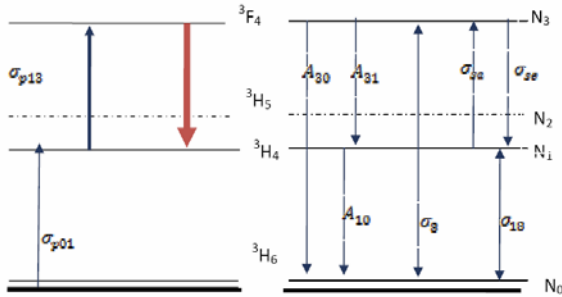

Fig. 4. Pumping mechanism of a 1420nm pumped TDFA (a) absorption or pump transitions (b) signal and ASE emission transitions. [9].

$$W_{p01,p13,p31} = \lambda_P \sigma_{p01,p13,p31} \left(\frac{P_P^+}{hcA_{eff}} \right) \tag{5}$$

$$W_{8a,8e,18a,18e} = \lambda_{ASE}^{8,18} \sigma_{8a,8e,18a,18e} \left(\frac{P_{ASE}^{8,18+} + P_{ASE}^{8,18-}}{hcA_{eff}} \right) \tag{6}$$

$$W_{sa,se} = \lambda \sigma_{sa,se} \left(\frac{P_{ASE}^+ + P_{ASE}^-}{hcA_{eff}} \right) + \lambda_s \sigma_{sa,se} \left(\frac{P_s}{hcA_{eff}} \right) \tag{7}$$

where σ is the absorption cross-section, h is a plank constant, A_{eff} is the effective area of the TDF. P_p, P_s and P_{ase} are the pump, signal and ASE powers respectively.

The light-wave propagation along the doped fiber in the z-direction can be established as follows:

$$\frac{dP_P^{\pm}}{dz} = \mp \Gamma(\lambda_{p1})(\sigma_{p13}N_3 - \sigma_{p01}N_1) \times P_P^{\pm} \mp \alpha P_P^{\pm} \tag{8}$$

$$\frac{dP_s}{dz} = \Gamma(\lambda_s)(\sigma_{se}(\lambda_s)N_3 - \sigma_{sa}(\lambda_s)N_1) \times dP_s - \alpha P_s \tag{9}$$

$$\frac{dP_{ASE}^{\pm}}{dz} = \pm \Gamma(\lambda_{ase})(\sigma_{se}(\lambda_{ase})N_3 - \sigma_{sa}(\lambda_{ase})N_1) \times P_{ASE}^{\pm} \pm \Gamma(\lambda_{ase})$$
$$(2h\nu\Delta\nu\sigma_{se}(\lambda_{ase})N_3) \mp \alpha P_{ASE}^{\pm} \tag{10}$$

$$\frac{dP_{ASE}^{8\pm}}{dz} = \pm \Gamma(\lambda_8)(\sigma_{8e}(\lambda_8)N_3 - \sigma_{8a}(\lambda_8)N_0) \times P_{ASE}^{8\pm} \pm$$
$$\Gamma(\lambda_8)(2h\nu\Delta\nu\sigma_8(\lambda_8)N_3) \mp \alpha P_{ASE}^{8\pm} \tag{11}$$

$$\frac{dP_{ASE}^{18\pm}}{dz} = \pm \Gamma(\lambda_{18})(\sigma_{18e}(\lambda_{18})N_1 - \sigma_{18a}(\lambda_{18})N_3) \times P_{ASE}^{18\pm} \pm$$
$$\Gamma(\lambda_{18})(2h\nu\Delta\nu\sigma_{18}(\lambda_{18})N_1) \mp \alpha P_{ASE}^{18\pm} \tag{12}$$

where α is the background scattering loss, which is assumed to be constant for all wavelengths. λ_{ASE}, λ_{ASE8} and λ_{ASE18} are the signal wavelengths, 800 nm ASE and 1800 nm ASE respectively. The overlapping factors between each radiation and the fiber fundamental mode, $\Gamma(\lambda)$ can be expressed as [10-11]:

$$\Gamma(\lambda) = 1 - e^{-\frac{2b^2}{\omega_0^2}} \tag{13}$$

$$\omega_0 = a\left(0.761 + \frac{1.237}{V^{1.5}} + \frac{1.429}{V^6} \right) \tag{14}$$

where ω_0 is the mode field radius defined by equation (14), a is the core diameter, b is the thulium ion-dopant radius and V is the normalized frequency.

5. Mathematical model for fiber Raman amplifier (FRA)

In order to obtain Raman amplification, a large pump wave power must be launched into the gain medium at a lower frequency to generate a stimulated Raman scattering (SRS) at a longer wavelength region. Raman gain depends on the amount of pump power and the frequency offset between pump source and signal. Amplification occurs when the lower frequency pumping photons transfers their energy to new high frequency photons at the signal wavelength. For a single signal, the pump power threshold that is required to achieve the SRS is given by [14]:

$$P_{th} = \frac{16 A_{eff}}{K_p L_{eff} g_r} \tag{15}$$

where K_p is the polarization constant which is around 2. A_{eff} and L_{eff} are the effective area and length of SMF fiber respectively. The overall Raman gain can be expressed in terms of the pump power and pump intensity as

$$g(v) = g_r(v)I_p = g_r(v)\frac{P_p}{A_{eff}} \qquad (16)$$

Above equation shows that gain is depending on the pump wavelength and pump power. In the steady state condition interaction between the pump and signal pumps as well as a backward pump powers and signal powers during the SRS process are governed by the following equation [15].

$$\pm\frac{dP_i}{dz} = \left[-\alpha_i + \sum_{j=1}^{i-1}\frac{gR(v_j-v_i)}{\Gamma Aeff}P_j - \sum_{j=i+1}^{m}\frac{v_i}{v_j}\frac{gR(v_i-v_j)}{\Gamma Aeff}P_j\right]P_i \qquad (17)$$

where z is signal propagation direction, A_{eff} is effective area of the Raman fiber as well as α_i account for attenuation coefficient for the i_{th} wave, respectively. The forward and backward signal propagation along the fiber is shown by plus and minus signs. In SRS process, the pump power provides the energy for amplification and depletes as the pump signal propagates along the fiber. Therefore, the gain reduces as the pump signal transfer all of its energy to input signal power, which resulted in gain saturation. The power along the length of the fiber is also reduced by the fiber losses, which occur in the medium due to its intrinsic properties. However, in case of bidirectional pumping, the coupled equation can be slightly more complicated because of two pump lasers. Due to tremendous calculation, the interaction of signal to signal was ignored, so by the help of equation (17) the pump power evolution in the fiber for the bidirectional FRA is described by [14]:

$$P_p(z) = P_{P\_in}\{r_f e^{-\alpha_p L(z)} + (1+r_f)e^{-\alpha_p(L-L(z))}\} \qquad (18)$$

where r_f is the ratio of the amount pump power launched in forward direction compared to the total pump power and it varies from 0 to 1. Using this equation, the signal intensity evolution in the fiber can also be described as:

$$\frac{dP_s}{dz} = \frac{g_r}{A_{eff}}P_{P\_in}^{\pm}e^{-\alpha_{ps}}P_s - \alpha_s P_s \qquad (19)$$

By solving this equation, we obtain

$$P_{s(z)} = P_{s\_in(z)}e^{\frac{gR e^{\pm}_{in}}{A_{eff}(-\alpha_p)}(e^{-\alpha_p z}-L)-\alpha_s z} \qquad (20)$$

Rayleigh scattering is one of the most important phenomena that limit the performance of Raman amplifier. Rayleigh scattering cause small parts of light back scattered. Normally, this Rayleigh back scattering is negligible. However in FRA this scattering may be amplified over a long length of transmission fiber by the Raman pump and affects the amplification performance in

two ways. Firstly, double Rayleigh scattering of the signal in optical fiber creates a crosstalk component in the forward direction and secondly, backward propagating noise part appears in the forward direction and enhancing the noise figure. The noise figure is strongly dependent on the ASE power [14]. The ASE power in the transmission fiber is given by:

$$P_{ASE} = \eta_{sp}(G_r-1)hV_sB_0 \qquad (21)$$

where, h is Planks constant, V_s is signal frequency, B_0 is the electrical bandwidth and η_{sp} is the spontaneous emission and calculated as:

$$\eta_{sp} = \frac{\eta N_3}{\eta N_3 - N_2} \quad , \text{where } \eta = \frac{\sigma_{SE}}{\sigma_{SA}} \qquad (22)$$

6. Numerical simulation

The theoretical results of hybrid amplifiers are obtained by solving the rate equations of the pump, signal power and ASE using a numerical method. *ode45* built in Matlab function was used to solve the numerical equations. The variable used in the numerical calculation and their corresponding values are shown in Tables 1 and 2 for the TDFA and FRA, respectively, which were obtained from various publications [8, 12, 14, 15].

Table 1. Numerical parameter used in the TDFA's simulation.

Parameter	Unit	Symb	Value
Thulium concentration	$1/m^3$	ρ	1.68×10^{25}
Numerical aperture		NA	0.3
Fiber Length	m	L	20
Background lost	dB/m	α	1.68×10^{25}
Effective area	m^2	A_{eff}	2.096×10^{-12}
Division along fiber			12
800nm ASE bandwidth	nm	Δv_8	10
1800nm ASE bandwidth	nm	Δv_{18}	100
ASE bandwidth	nm	Δv	2
Signal absorption cross	m^2	σ_{sa}	Maccamber
Signal stimulated	m^2	σ_{se}	Fig.2
800nm transition cross	m^2	$\sigma_{03,}$	6.2×10^{-25}
1800nm transition cross	m^2	$\sigma_{01,}$	5.2×10^{-25}
Radiative decay rate	1/s	A_{10}	172.4
Radiative decay rate	1/s	A_{30}	702.8
Radiative decay rate	1/s	A_{50}	676.3
Radiative decay rate	1/s	A_{52}	492.9
Nonadiative decay rate	1/s	A_{43}^{nr}	52976
Nonadiative decay rate	1/s	A_{21}^{nr}	165626

Table 2. Numerical parameter used in the FRA's simulation.

Parameter	Unit	Symbol	Value
Numerical aperture		NA	0.3
Fiber Length	Km	L	12
Background lost	dB/m	α	1.68×10^{25}
Effective area	m^2	Aeff	70e-12
Signal wavelength	nm	λs	1550
Pump wavelength	nm	λp	1420
Input signal Power	nm	P_{s_in}	0.1
Raman Gain	m/W	g_R	1.0324886e-

7. Results and discussion

Fig. 5 shows the calculated fractional inversion as a function of longitudinal position along the TDF, where curve (a) shows the result corresponds to a1420 nm pumped with 6000 ppm concentration. Fractional inversion is nearly unity (0.6) at the first meter of the fiber and then decrease to 0.3 at 4 miter long fiber. Note that the 1420 nm-pumped TDFA with low concentration 2000 ppm has a very high fractional inversion of nearly unity (0.95) in the whole position as shown in curve b of Fig. 5. From these results, we consider the numerical modeling of the gain shifted TDFA to be successful.
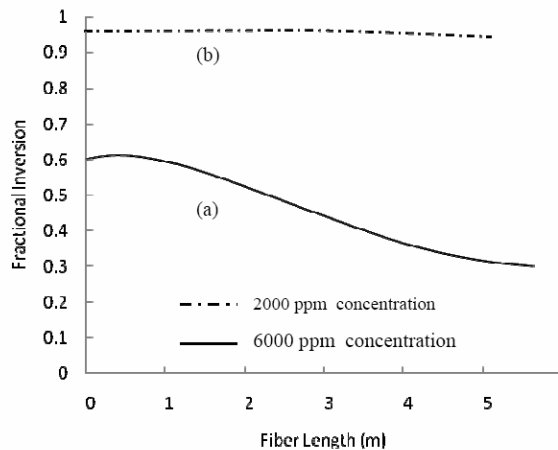

Fig. 5. Fractional inversion as a function of length.

Fig. 6 shows the gain spectra of a wide-band hybrid low concentration TDFA and Raman amplifier and the individual TDFA and FRA. In this experiment, the 1420nm pump powers were fixed at 250 mW and 550 mW for the TDF and DCF, respectively. The peaks of both TDFA and FRA gains are obtained at 1460 nm and 1530 nm, respectively with peak power of around 24dB as shown in the Fig. 6. The superposition of these gain spectra by the hybrid amplifier has significantly wider the gain bandwidth. For achieving the gain flattened hybrid, the gap between the two peaks must be compensated by shifting the gain spectrum of the TDFA to a longer

wavelength. Fig. 7 shows the gain spectrum of the proposed hybrid amplifier with two-stage TDFA compared with the individual first stage TDFA, second stage TDFA and the third stage FRA. As shown in Fig. 7, a relatively flat gain spectrum is obtained without any gain equalizer by the single-wavelength pumping approach in the proposed hybrid amplifier. The theoretical results are also compared with the experimental results as shown in Figs. 6 and 7. As shown in both figures, the theoretical results are in good agreement with the experimental results, which indicates the accuracy of our modeling.

The gain variation to gain ratio ΔG/G is generally used to characterize the gain variation, where ΔG and G are the gain excursion and the average gain value, respectively [16]. In order to define the gain flatness of amplifier, the ΔG/G for the TDFA and Raman fiber hybrid amplifier with and without high concentration is compared between 1460 and 1535 nm under the same condition. The gain variation ΔG/G for the proposed hybrid amplifier was calculated to be around 0.05 (1.3 dB / 24.14 dB) that is 70 % better than a conventional hybrid amplifier without high concentration TDF, which has the gain variation of 0.17 (4.2 dB / 24.14 dB) [16].
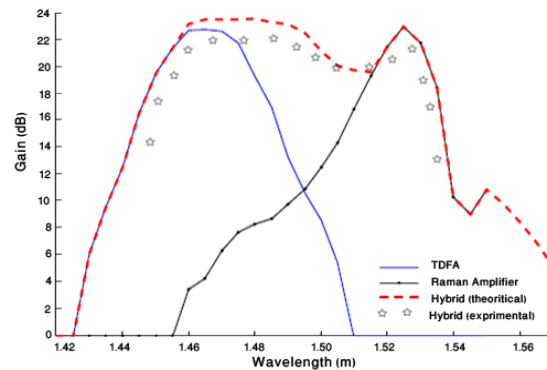

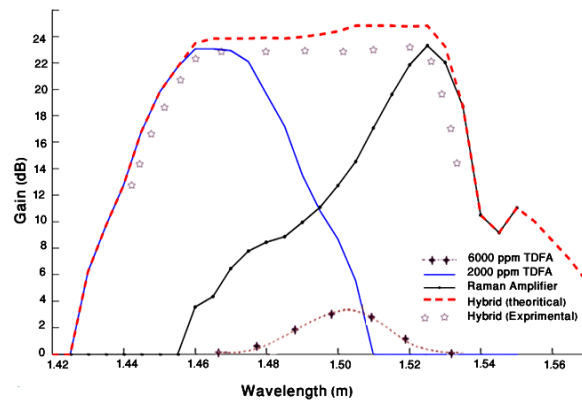*Fig. 6. Gain spectrum of the conventional hybrid amplifier compared with the individual gains for TDFA and FRA.*

Fig. 7. Gain spectrum of the proposed hybrid amplifier compared with the individual gains for single-stage TDFA, second stage TDFA and FRA

8. Conclusion

In this paper, the hybrid amplifier is proposed using a series configuration of two-stage TDFA and Raman amplifier, which sharing the same pump laser. Cascading of fiber Raman amplifier and TDFA gain spectrum has covered the entire S-band region. The flat gain is obtained at around 24 dB by the help of second stage TDFA with a high Thulium concentration TDF. Therefore this approach is very promising and can be used for the development of wide-band hybrid amplifiers in the S-band region. The development of reliable high-power diode lasers in the 1420 nm wavelength range will make this type of wide-band hybrid amplifier an interesting candidate for S-band optical telecommunication systems.

References

[1] S. W. Harun, F. A. Rahman, K. Dimyati, H. Ahmad, Laser Phys. Lett., **3**(11), 536 (2006).

[2] S. W. Harun, N. Tamchek, P. Poopalan, H. Ahmad, Jap. J. Appl. Phys. Pt. 2, **41**, (3B), L332 (2002).

[3] S. W. Harun, N. K. Saat, H. Ahmad, IEICE Electronics Express, **2**(6), 182 (2005).

[4] Y. Miyamoto, H. Masuda, A. Hirano, S. Kuwahara, Y. Kisaka, H. Kawakami, M. Tomizawa, Y. Tada, S. Aozasa Electron. Letter, **38**(24), 1569 (2002).

[5] T. Sakamoto, S. Aozasa , M. Yamada, M. Shimizu, IEEE J. of Lightwave Technology, **24**(6), 2287 (2002).

[6] S. R. Luthi, G. F. Guimaraes, J. Freitas, A. Gomes, Quantum Electronics and Laser Science Conference, 2006, pp: 1 – 2.

[7] G. F. Guimarares, S. R. Luthi, J. F. L. Freitas, A. S. L. Gomes, Electron. Letters, **42**, 997 (2006).

[8] S. S. H. Yam, J. Kim, M.E. Marhic, Y. Akasaka, L. G. Kazovsky, IEEE Photonics Technology Letters, **16**(7), 1646 (2004).

[9] P. Peterka, B. Faure, W. Blance, M. Karasek, J. Optical and Quantum Electron., **36**, 201 (2004).

[10] M. Eichhorn, J. Quantum Electronics **41**(12), 1574 (2005).

[11] E. Desurvire, John Wiley & Son, New York, 1994.

[12] M. Karasek, J. Quantum Electronics, **33**(10), 1699 (1997).

[13] S. S. H. Yam, J. Kim, Selected Topics in Quantum Electronics, **12**(4), 797 (2006).

[14] Mohammed N. Islam, "Raman Amplifiers for Telecommunications 1: Physical Principles," Springer, December 2003.

[15] L. Xueming , L. Byoungho EEE Photonics Technology Letters **16**(2), 428 (2004).

[16] U. –C. Ryu, K. Oh, W. Shin, U. C. Paek, IEEE J. of Quantum Electron., **38**, 149 (2002).

---

[*]Corresponding author: swharun@um.edu.my; S.D.Emami@gmail.com